On the shear band velocity in metallic glasses: a high-speed imaging study

M. Seleznev[1], I. S. Yasnikov[2], A. Vinogradov[3]

[1] Freiberg University of Mining and Technology, Freiberg, 09599, Germany

[2] Institute of Advanced Technologies, Togliatti State University, 445020, Russia

[3] Norwegian University of Science and Technology – NTNU, Trondheim, 7491, Norway

Development of localised shear bands (SB) in bulk metallic glassy (BMG) alloys was investigated by a high-speed microscopic imaging technique. The velocities of SBs propagating by a progressive mechanism were found to be in the m/s range. It has been shown that after rapid initiation, the mean SB velocity decays as a function of time *t*, exhibiting a scaling-like t^{-n} behaviour with *n* close to 2 over several orders of magnitude.

Keywords: metallic glasses; shear bands; velocity; rapid video imaging

Metallic glasses (MGs) possess high strength while their ductility at low homologous temperature is low. Plastic deformation of MGs is confined to narrow, of 10 nm wide, shear bands (SBs) [1, 2]. Once initiated, a shear band dominates the plastic strain distribution and the plastic strain rate, which is by orders of magnitude higher than the imposed strain rate. Due to apparent lack of work hardening, rapid shear strain localisation in SBs greatly destabilizes plastic flow and provokes early development of micro-cracks leading finally to catastrophic fracture [3, 4]. Although the SBs in MGs have been intensively studied during past three decades, the phenomenology of shear banding and its underlying microscopic mechanism in MGs is still unclear [1, 5]. Experimental investigations of SB dynamics are still challenging in view of their nano-scale spatial dimensions (thickness) and rapid temporal evolution [2, 5].

Considerable evidence exists to suggest that under quasi-static loading, shear-banding events initiate heterogeneously at stress concentrations at the surface. The shear front propagates across the specimen, disordering the atomic structure along its path [6], changing the internal stress distribution [7, 8], lowering the local flow stress, and finally promoting continued progressive deformation along the resulting macroscopic SB [2, 9].

The significantly different results have been reported for the SB velocity, depending on the experimental technique used. On large time scales corresponding to stress drops caused by continuously propagating SBs, the SB velocity can be measured with a high accuracy [10] (see

excellent surveys by Song and Nieh [9] and by Maaß and Löffler [5]). The peak velocity is attained at about half the stress-drop event. Depending on temperature, it varies from 10^{-6} m/s to 10^{-2} m/s [9-12]. This is far too small to be detected by the acoustic emission (AE) technique [13]. AE accompanies the stress drops, even the finest ones, and shows that the SB initiates with significantly higher velocities [13, 14]. Based on molecular dynamic simulations, Shimizu et al. [15] predicted that the nucleating shear front should propagate at approximately the shear wave speed C_S. Using a high speed (up to 2×10^6 fps) cinematography Tabachnikova et al. [16] have shown that SB initiation followed by fracture in melt-span MG ribbons occurs within a few microseconds in fair agreement with AE-based estimates of initiation time [13, 14]. Then, a macroscopic SB propagates at about $1\text{-}2\times10^3$ m/s (that is actually close to a terminal velocity C_S), the offset increases and a mode II shear crack initiates [3] resulting in rapid failure. Wright et al. [10] have also observed that system-spanning SB propagation and fracture occur at substantially different time scales. A lower bound velocity for the development of fracture was found to be of 170 m/s. A simultaneous slip is only possible along a fully developed SB. However, the developing of a major SB itself is believed to occur in a progressive manner [17, 18].

In-situ observations of the SBs in MGs are still surprisingly scarce. The present brief communication is focused on characterisation of the behaviour of the non-system-spanning SBs and on evaluation of their velocity after rapid initiation.

The samples of the rapidly solidified $Pd_{40}Cu_{30}Ni_{10}P_{20}$ and $Pd_{40}Ni_{40}P_{20}$ BMGs with $5.5\times2.7\times2.7$ mm^3 and $10\times2\times1$ mm^3 dimensions, respectively, for compression and three-point bending testing were cut by spark-erosion. The 2:1 aspect ratio of the compression specimens was chosen to avoid buckling instability. The side notch with of 1 mm radius was introduced into the specimen to localise the shearing area in the field of view and to prevent shear front propagation through the whole sample. The specimen surface was polished to the mirror-like finish. The experimental setup was described in detail in [19]. The exact specimen geometry, imposed load and typical shear band patterns are shown in Fig.S1 in Supplemental Material providing additional methodological details. The loading conditions and the observed shear geometry resemble closely those discussed in [20]. A screw-driven rigid testing machine (Kammrath&Weiss) was used for loading in compression with the crosshead speed 1 μm/s. The imaging system comprises of a high-speed Photron-SA3 camera equipped with the Navitar-6000 microscopic lens. The camera operated at different rates from 6000 to 30000 fps. To capture the sudden shear events, the camera was triggered by the homemade AE-based feedback

circuit. When a shear event, e.g. such as those shown in Fig.1, occurs, the AE signal is generated. This signal triggers the camera to stop video capturing. The capacity of the optical video imaging system to resolve the finest details of the SB morphology was assessed by using the scanning white-light interferometry as discussed in Supplemental Material. Successive grayscale video frames were processed using a pixel subtraction algorithm, where the regions experiencing shear displacements are marked as white areas leaving plastically undeformed regions in black. Not only this permitted accurate tracking of the front of the propagating band even when the displacements along a band are variable but also helped distinguishing between different possible scenarios of SB propagation reviewed in detail in [20] and illustrated schematically in Fig.1: when the SB initiates at the middle (a) or at the edge (b,c) of the specimen; when the shear front is "freshly" nucleated (c) or it propagates along the "pre-existing" (b) one. Once initiated, the shear band defines a plane on which slip is more easily accommodated than in the bulk of the material. Direct observations show that regardless of the history depicted in Fig.1, the shear front propagates in a progressive manner. Comparison of the behaviour of the "fresh" SB (Fig.1c) with that propagating along the "pre-existing" one (Fig.1b) shows no significant difference in the shear front path or in the calculated shear front velocities. Thus, independently of the shear prehistory, every SB behaves like a newly formed one. The mean propagation speed of the shear front was estimated by dividing the increment of the shear band length ΔL, which was observed on the surface within one frame, to the time interval Δt between the frames. The shear events were observed within at least two-three successive frames. More than 200 shear events were captured and analysed in this way.

The mean propagation speed of the shear front was estimated to be of 1-5 m/s which is substantially higher than that for the continuous shear slippage (10^{-4}×10^{-3} m/s [5, 9]), but is still much smaller than that expected for rapid shear band initiation and fracture (>170 m/s [10]). Figure 2 shows the graph compiling the results of present direct video observations and data reported in the literature for the non-system-spanning SBs and the SBs evolving to the final mode II fracture. The consensus exists in literature that fracture in a ductile BMG occurs within a dominant SB serving as a precursor of imminent localised fracture [1-4, 21]. Traces of SBs on fractured surfaces were also found in [16]. Therefore, it can be reasonably assumed that shear crack initiation and growth preceded by shear front propagation. Accordingly, shear crack front velocity data can be considered as upper bound estimates of the velocity of the shear front initiated just before the catastrophic failure (see also [22] where this two stage process has been resolved temporarily by the AE technique). A most intriguing result of the present work is that,

within a reasonable scatter, all data points align themselves approximately in a straight line (in log-log coordinates) demonstrating ~t^{-n} scaling with exponent n approximately equal to 2 over a wide range of t within a reasonably compact scatter band.

It is obvious that every possible shearing process starts and ends with zero velocity, i.e. the time dependence of the velocity profile has a pronounced maximum [2, 5] (see a schematic inset in Fig.2). Depending on the applied stress and deformation prehistory, the propagating shear front can evolve in two ways, resembling the bifurcation behaviour around a critical point, Fig.2: (i) nucleation of a shear crack and its rapid propagation to failure (ii) shear front deceleration and termination inside the specimen. As opposes to the symmetrical velocity profile observed commonly in a major shear band on the stage of continuous shear sliding [1, 2, 9-12], the evidence is seen that after rapid initiation within few microseconds [14, 23] up the maximum velocity V_{max} at τ_i, the SB propagates through the specimen with the gradually decreasing velocity obeying the t^{-2} relation until a complete stop at $\tau_f >> \tau_i$ (with τ_f being in the millisecond range). The initiation stage is accompanied by a strong transient AE signal, while no AE is detected during the deceleration stage [14, 24]. To highlight that the decelerating behaviour of the SB was properly captured, several data points corresponding to the successive stages of the same shearing events are connected by solid lines in Fig.2 (green and pink lines for two glasses, correspondingly). It is clear that these lines obey the general t^{-2} trend.

Based on experimental observations, the phenomenological behaviour of the average SB velocity can be expressed as

$$\langle V(t)\rangle = \frac{\Delta L}{\Delta t} = \frac{k}{t^2} \tag{1}$$

with k - a constant characterising the slope of the $\langle V\rangle$ vs. t line, and, hence, we obtain $\Delta L = \frac{k\Delta t}{t^2} = \Delta\left(\frac{k}{t}\right)$. Passing to infinitesimal increments and integrating with the boundary condition $L(t\to\infty) = L_S$ with L_S - the size of the specimen, which determines the maximum possible SB length, yields the following time dependence of the SB length

$$L(t) = L_S - \frac{k}{t} \tag{2}$$

The k value can be estimated from the following considerations. The upper most points on the graph, Fig.2, correspond to the case when the major shear band followed by mode II fracture

initiates at the edge of the ribbon-shaped metallic glasses and spans the specimens at the velocity close to the velocity of sound [16]. For the given specimen dimensions (L_S =5-6 mm) and estimations of the SB velocity of 1.0×10^3 (average) and 2.2×10^3 m/s (maximum) made in [16], one obtains $k = \langle V \rangle t^2 = \langle V \rangle \cdot \left(\frac{L_S}{\langle V \rangle} \right)^2 = 2 - 5\times10^{-9}\ m \cdot s$. In the lower bound estimate, k is approximately equal to L_S^2 / C_S. From Fig.2 one can easily see that the experimental data obtained in the present work are nicely accounted for by the proposed empiric relation (1) with the above estimated k.

In summary, using a high-speed imaging system it was shown that:

- the SB initiates heterogeneously and propagates in a progressive manner until it passes through the specimen or terminates inside;

- after rapid initiation within few microseconds, the SB propagates with decaying velocity which can be approximated by the t^{-2} scaling function;

- not only this accounts for the SB velocities measured in the range of 10^1-5×10^{-2} m/s after a few milliseconds from initiation, but also explains a wide range of experimental data reported in the literature for SB velocities in metallic glasses.

As a future scope of this work, a more elaborated phenomenological model of the dynamics of shear bands and their bifurcation-like behaviour in metallic glasses will be presented elsewhere along with the detailed results of the literature survey including experimental data for measurements of velocities of the slow system spanning slippage in major shear bands.

MS is grateful to the Materials Physics department, the University of Muenster (Prof. G. Wilde group) for the opportunity to use BMG samples cast in their laboratory. IY acknowledges financial support from the Russian Foundation for Basic Research (RFBR) under Project no. 18-08-00327.

References

[1] A.L. Greer, Y.Q. Cheng, E. Ma, Mater. Sci. Eng. R 74 (2013) 71-132.
[2] T.C. Hufnagel, C.A. Schuh, M.L. Falk, Acta Materialia 109 (2016) 375-393.
[3] P.G. Zielinski, D.G. Ast, Philosophical Magazine A 48 (1983) 811-824.
[4] Y.-Y. Zhao, G. Zhang, D. Estévez, C.I. Chang, X.D. Wang, R.-W. Li, J. of Alloys and Compounds 621 (2015) 238-243.
[5] R. Maaß, J.F. Löffler, Advanced Functional Materials 25 (2015) 2353-2368.
[6] H. Rösner, M. Peterlechner, C. Kübel, V. Schmidt, G. Wilde, Ultramicroscopy 142 (2014) 1-9.
[7] R. Maaß, P. Birckigt, C. Borchers, K. Samwer, C.A. Volkert, Acta Materialia 98 (2015) 94-102.
[8] A. Vinogradov, M. Seleznev, I.S. Yasnikov, Scripta Materialia 130 (2017) 138-142.
[9] S.X. Song, T.G. Nieh, Intermetallics 19 (2011) 1968-1977.
[10] W.J. Wright, R.R. Byer, X. Gu, Applied Physics Letters 102 (2013) 241920-4.
[11] R. Maaß, D. Klaumünzer, J.F. Löffler, Acta Materialia 59 (2011) 3205-3213.
[12] P. Thurnheer, R. Maaß, K.J. Laws, S. Pogatscher, J.F. Löffler, Acta Materialia 96 (2015) 428-436.
[13] A. Vinogradov, Scripta Materialia 63 (2010) 89-92.
[14] D. Klaumünzer, A. Lazarev, R. Maaß, F.H. Dalla Torre, A. Vinogradov, J.F. Löffler, Phys. Rev. Letters 107 (2011) 185502.
[15] F. Shimizu, S. Ogata, J. Li,, Acta Materialia 54 (2006) 4293-4298.
[16] E.D. Tabachnikova, Y.I. Golovin, M.V. Makarov, A.A. Shibkov, Journal De Physique. IV 7 (1997) C3-307-C3-310.
[17] R.T. Qu, Z.Q. Liu, G. Wang, Z.F. Zhang, Acta Materialia 91 (2015) 19-33.
[18] A.J. Cao, Y.Q. Cheng, E. Ma, Acta Materialia 57 (2009) 5146-5155.
[19] M. Seleznev, A. Vinogradov, Review of Scientific Instruments 85 (2014) 076103.
[20] D.B. Miracle, A. Concustell, Y. Zhang, A.R. Yavari, A.L. Greer, Acta Materialia 59 (2011) 2831-2840.
[21] R. Narasimhan, P. Tandaiya, I. Singh, R.L. Narayan, U. Ramamurty, Int. J. of Fracture 191 (2015) 53-75.
[22] A.Y. Vinogradov, V.A. Khonik, Philosophical Magazine 84 (2004) 2147-2166.
[23] D. Klaumünzer, R. Maaß, J.F. Löffler, Journal of Materials Research 26 (2011) 1453-1463.
[24] W.J. Wright, Y. Liu, X. Gu, K.D. Van Ness, S.L. Robare, X. Liu, J. Antonaglia, M. LeBlanc, J.T. Uhl, T.C. Hufnagel, K.A. Dahmen, Journal of Applied Physics 119 (2016) 084908.

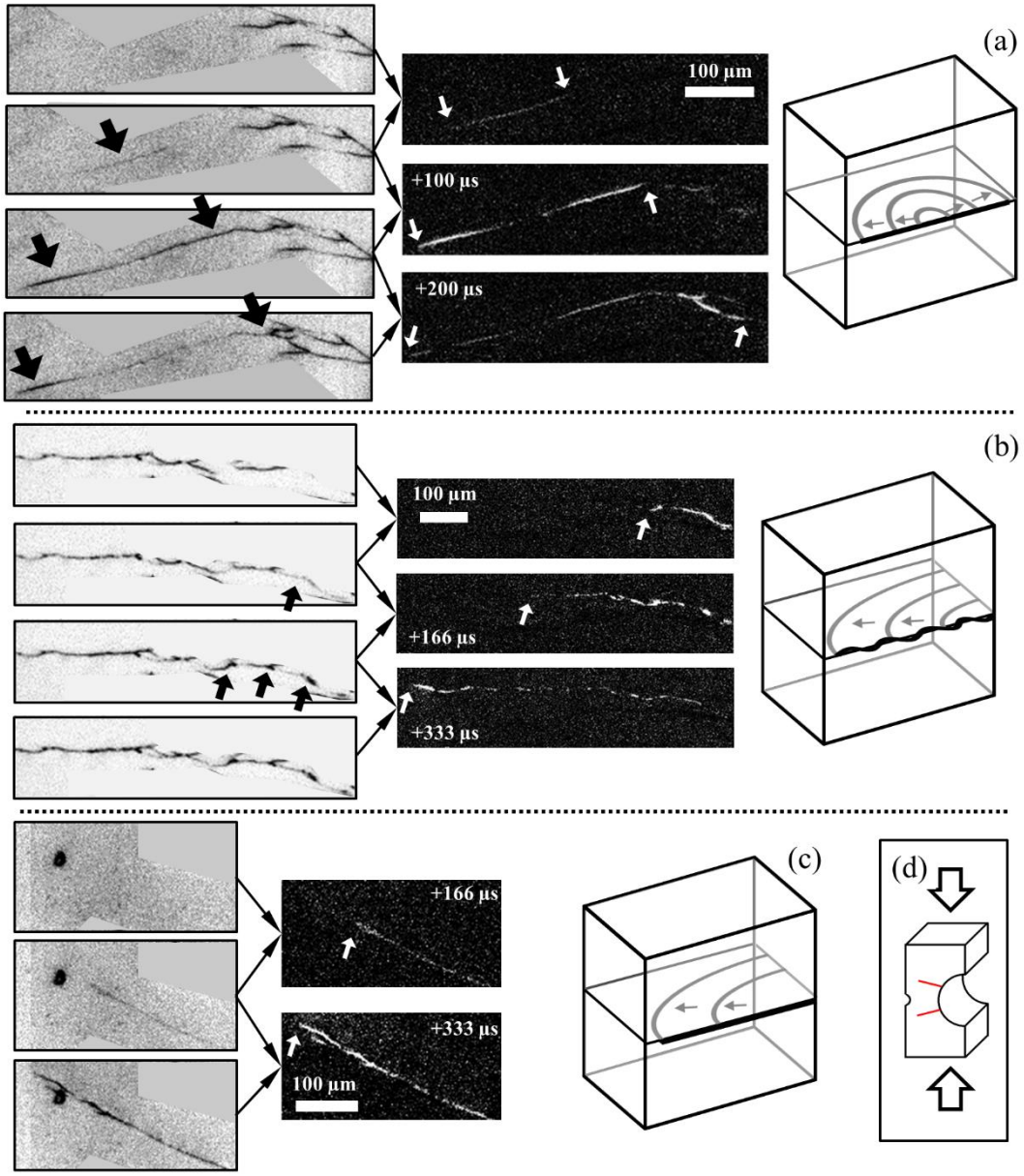

Figure 1. Typical examples of high-speed video images illustrating shear band propagation from the face (a) or the edge (b) in the Pd-based BMG. The left column shows the as-captured successive frames from top to bottom; arrows indicate shear development. Images in the centre represent the results of subtraction of two subsequent frames. White arrows indicate the shear tip position; the number indicates the time elapsed between the frames in μs. Drawings to the right show schematics of shear front propagation corresponding to observations. A schematic of a specimen shape and loading direction is given in (d), showing the applied force (arrows) and SBs initiation from the notch.

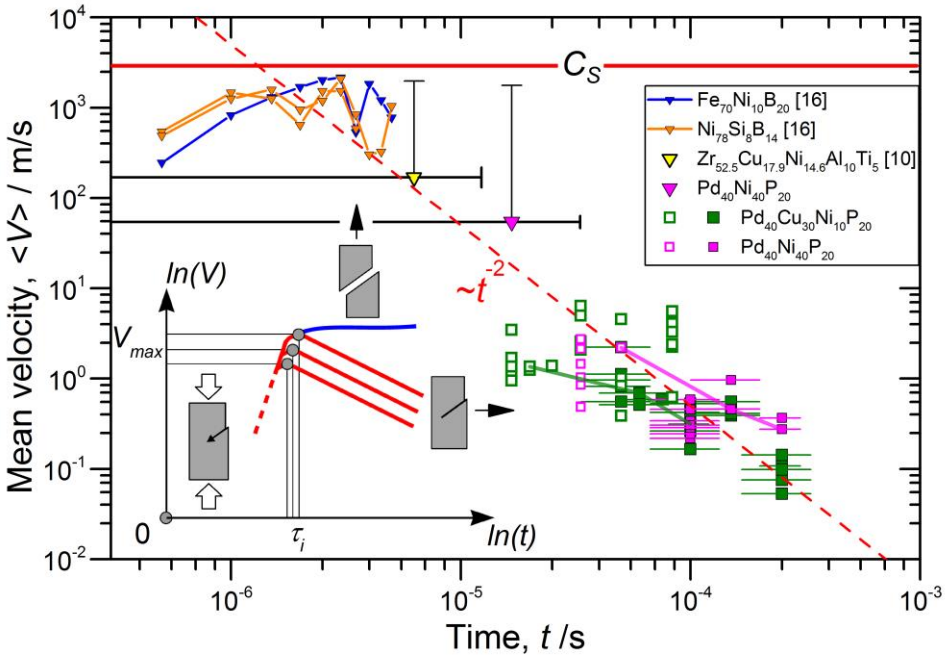

Figure 2. Distribution of experimentally obtained shear band velocities on different time scales during localised deformation in MGs. The schematics on the inset illustrates two possible scenario of shear front evolution towards either a mode II crack (triangles) and failure or a terminated SB (squares). Open squares correspond to velocities calculated from the first appearance of the shear front in the field of view. Solid lines connect the points corresponding to the same propagating shear front, highlighting the decelerating behaviour of the SB.